Design of a modern optical fibre spectral transmissometer and a 120° scattering meter

1998 J. Opt. 29 53

(http://iopscience.iop.org/0150-536X/29/2/001)

J. Opt. **29** (1998) 53–62. Printed in the UK PII: S0150-536X(98)90668-2

Design of a modern optical fibre spectral transmissometer and a 120° scattering meter

Othman H Y Zalloum†

Physics Department, University College Dublin, Belfield, Dublin 4, Ireland

Received 18 June 1997, accepted 7 January 1998

Abstract. This paper describes an *in situ* new technology optical fibre-based system designed to yield simultaneous measurements of the spectral attenuation coefficient, $c(\lambda)$, and the volume scattering function at 120° backwards on ocean waters, within the spectral range 400–800 nm. The volume scattering function at 120°, $\beta(120^\circ, \lambda)$, will be used to derive the backward scattering coefficient, $b_b(\lambda)$. Optical and mechanical designs are presented. The considerations leading to the design of the instrument, its capabilities and the unique features it incorporates are discussed. Methods for absolute calibration of the instrument are presented.

Keywords: Spectral measurements, underwater optics, volume scattering function, spectral attenuation coefficient

Schémas d'un moderne transmissometteur de spectrale à fibre optique et d'un metteur de diffusion angulaire de 120°

Résumé. Cet article décrit un nouveau systeme *in situ* basé sur la technologie des fibres optiques, destiné à mesurer simultanément le coefficient d'atténuation spectrale, $c(\lambda)$, et le coefficient angulaire de diffusion à 120° en arrière des eaux océaniques, dans le spectre de 400 nm à 800 nm. Le coefficient angulaire de diffusion à 120°, $\beta(120^\circ, \lambda)$, sera utilisé pour dériver le coefficient de diffusion arrière, $b_b(\lambda)$. Les schémas optiques et mécaniques sont présentées. Les considérations résidant au schéma de l'instrument, ses capacités et ses caractéristiques uniques sont discutées. Des méthodes pour un calibrage absolu de cet instrument sont présentées.

Mots clés: Mesures spectrales, optique sous-marine, coefficient angulaire de diffusion, coefficient d'atténuation spectrale

1. Introduction

The characterization of a body of water by optical means relies on a variety of different types of measurement [1, 2]. The beam attenuation coefficient, $c(\lambda)$, and the backward scattering coefficient, $b_b(\lambda)$, like other inherent optical properties, are of great significance in the study of radiative transfer, optical modelling and remote sensing applications [3–6]. Because $c(\lambda)$ and $b_b(\lambda)$ are inherent optical properties, both are important measurements in the optical characterization of a water sample. Any study of the inter-relationship of the inherent and apparent optical properties must involve both $c(\lambda)$ and $b_b(\lambda)$. The fact that each parameter is most sensitive to a different set of attributes suggests that much information about the nature of particles suspended in a body of water could be inferred from simultaneous measurements of the optical properties.

The beam attenuation coefficient, $c(\lambda)$, enters as an important parameter in the models of underwater visibility [7–9]. The inverse of the beam attenuation coefficient, the attenuation length, is important as a scaling parameter for problems in imaging. When calibrated correctly, $c(\lambda)$ can be used to determine the suspended particulate load in a water sample, since it is a sensitive indicator in the ultraviolet and the visible band of the light spectrum of the suspended particles and organic substances in the sea [10].

† Now at: Physics Department, Zarka University, PO Box (150863), Zarka 13115, Jordan.

0150-536X/98/020053+10$19.50

The vertical structure of the radiance distribution and hence irradiance depends on the beam attenuation coefficient and the scattering function.

The *in situ* transmittance meter has for a long time been an effective means of studying the optical properties especially of coastal waters [3, 11, 12]. If furnished with an adequate depth-sensing unit, the instrument yields records of transmittance as a function of depth even in rough weather. The meter must be highly efficient in excluding scattered light. The principles of design of the beam transmissometer and the variation of the size error with the design parameters have been discussed by Austin and Petzold [13] and by Voss and Austin [3]. Various designs which differ in technical details, features and capabilities have been reported [14–20].

Austin and Petzold [15] reported on an instrument that performs simultaneous measurements of the beam attenuation coefficient and the small-angle volume scattering function at three angles. Any ten wavelengths covering the spectral range from 400 to 670 nm may be used. The instrument reported by Borgerson *et al* [20] collects spectral attenuation data on command. A scan from 800 to 400 nm and back requires about 16 s. The solid spectral transmissometer and radiometer reported by Carder *et al* [16] employs a 256-channel, charge-coupled-type linear array measuring the spectral intensities diffracted by a grating from 400 to 750 nm. There are new spectral transmissometers that are commercially available now, these include, but are not limited to, the WETlabs AC-9 and AC-3. The AC-9 measures the spectral absorption and spectral attenuation coefficients over nine wavelengths via a dual-path measurement. It typically employs a 25 cm path length for the measurement of low attenuance by ocean water [21, 22]. WETlabs AC3 is a spectral transmissometer and absorption meter operating at 456, 488 and 532 nm [23].

The backward scattering coefficient enters into many issues concerned with the underwater light field [1], ocean colour spectrum and optical two-stream models such as irradiance reflectance, shape factors and irradiance backscattering coefficients [24–26]. The absorption and the backward scattering coefficients are believed to carry substantial information about the sea water. Information about these parameters is important in optical sensing and in radiative transfer modelling for developing algorithms to analyse remotely sensed spectral data.

The traditional methods to estimate the backward scattering coefficient requires irradiance measurements [25, 27] in the natural light field, or by direct integration of the measured volume scattering function from 90° to 180° in scattering angle [28]. Oishi [29] has shown by means of Mie scattering computations that one can estimate the backward scattering coefficient due to particles by observing the scattering at 120° using the following simple relation:

$$b_{\mathrm{bp}} = (6.9 \pm 0.4)\beta_{\mathrm{p}}(120^\circ) \qquad (1)$$

where b_{bp} and $\beta_{\mathrm{p}}(120^\circ)$ are the backward scattering coefficient and the volume scattering function at 120° due to particles, respectively. The *in situ* observations of scattering functions presented by Oishi [29] give a best fit at 120° with a regression line of $b_{\mathrm{b}} = 7.19 \times \beta(120^\circ) - 0.43 \times 10^{-4}$ m^{-1}. Equation (1) has been found to apply over a wide range of naturally occurring conditions, from clear oceanic waters to turbid estuarine waters with high concentration of particles and seems to hold for different wavelengths in the visible part of the spectrum.

The optical backscattering sensor in this study aims to measure scattered radiance at 120° from which $b_{\mathrm{b}}(\lambda)$ can be derived by applying either equation (1) or the above equation of the regression line.

Various investigators have reported on optical backscattering sensors [23, 30, 31]. The instrument of Maffione *et al* [30] measures $\beta(\theta)$ in the backward direction over a range of scattering angles from ∼115°–170°. The calibration of their sensor yields a weighted angular averaged value of $\beta(\theta)$ with a centroid located at a scattering angle of about 150°. In their investigations, Voss and Smart [23] used the APL backscattering sensor which measures the $\beta(170^\circ)$, the SRI Beta Pi sensor, which measures the $\beta(\theta)$ from 170° to 180° and the SRI backscattering sensor, which measures $\beta(150^\circ)$. The Southampton Underwater Multi-parameter Optical Spectrometer System (SUMOSS) reported by Schwartz *et al* [31] measures up- and downwelling irradiance, beam transmission and forward, side and backward scatter. It is an instrument for the simultaneous *in situ* measurements of inherent and apparent optical properties which employs a two-dimensional CCD detector array.

2. Present design requirements

The present work has been carried out by the author as a component for the development of the Marine Radiometric Spectrometer (MARAS). The MARAS system (including the active suites, see below) is a novel instrument system designed by a team of research scientists [32–35] in the Physics Department at University College Dublin which allows for the first time a complete spectral characterization of the optical properties of marine waters. The recent results of O'Mongain *et al* [2] demonstrate the capacity of *in situ* full spectral radiometry using MARAS for characterizing the optical properties of marine waters over the spectral range 400–800 nm with a nominal resolution of 4 nm.

MARAS is based on the following inter-related principle elements:

- optical collectors (passive and active suites) for the various radiometric quantities to be measured;
- a multi-input spectrometer with an imaging detector; a CCD camera;
- analogue video equipped with an image framegrabber;
- data acquisition and processing software.

Among the parameters which are to be measured by MARAS collectors are:

(i) path transmissivity for determining the spectral beam attenuation coefficient, $c(\lambda)$. This requires two collectors, one to monitor the light source;
(ii) scattered spectral radiance at 120°, from which $\beta(120^\circ)$ can be determined from the derivation of the backward scattering coefficient $b_{\mathrm{b}}(\lambda)$.

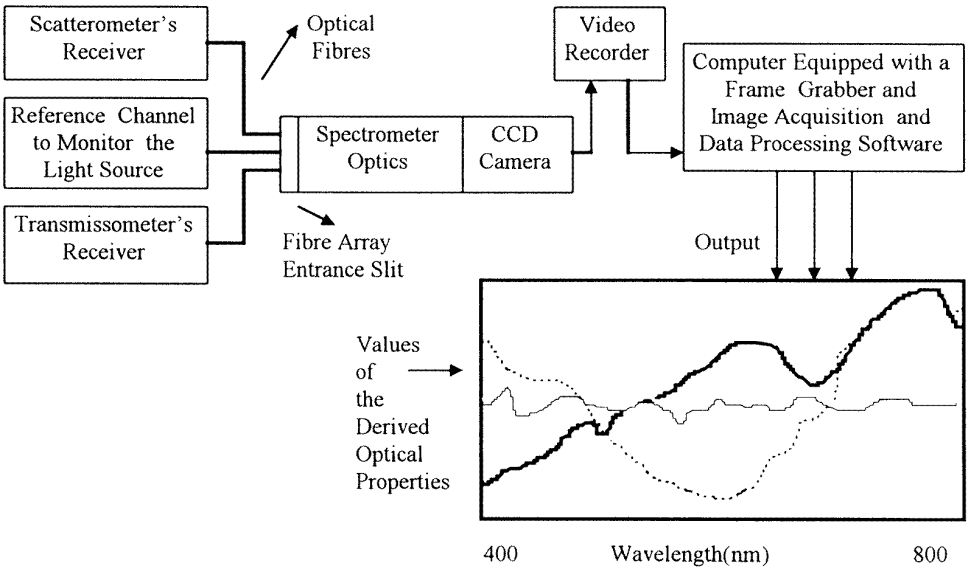

Figure 1. A block diagram of the complete system using only three input channels of the multi-input spectrometer. Seven additional channels can be accommodated at the fibre array entrance slit of the spectrometer corresponding to seven more optical collectors for other radiometric quantities to be measured in the marine environment.

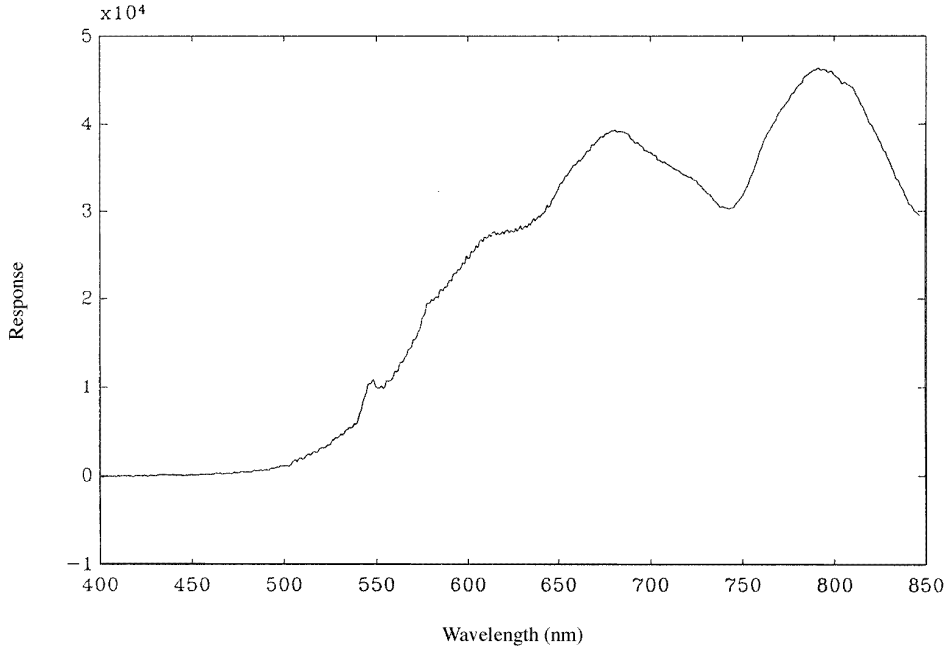

Figure 2. A typical integrated reference signal from a tungsten light source with mean integrated dark current subtracted.

The active suite, the spectral transmissometer and the 120° spectral scatterometer, of interest here, have been designed by the author to be integrated with a multi-input submersible spectrometer. The submersible spectrometer and the passive suite (various optical collectors for other radiometric quantities to be measured, not described here) have been designed, developed and tested by independent research [32, 33, 35].

The spectrometer images the whole spectrum from each collector simultaneously onto a two-dimensional CCD. The CCD array detector is mounted in a standard CCIR video system. Thus all data can be readily recorded and replayed using VHS analogue TV technology. The CCD array detector allows simultaneous multiple spectra from all the sensors to be recorded and transmits all data as a video signal for on-board recording and processing. The 25 Hz sampling of the TV system is turned to an advantage by using a computer-controlled framegrabber to digitize the signal and to integrate by frame addition in computer memory. Data are stored on a standard analogue video tape and are processed by a computer equipped with an image framegrabber using advanced frame-grabbing techniques and specially adapted versions of data acquisition and image processing software. The optical collectors, spectrometer

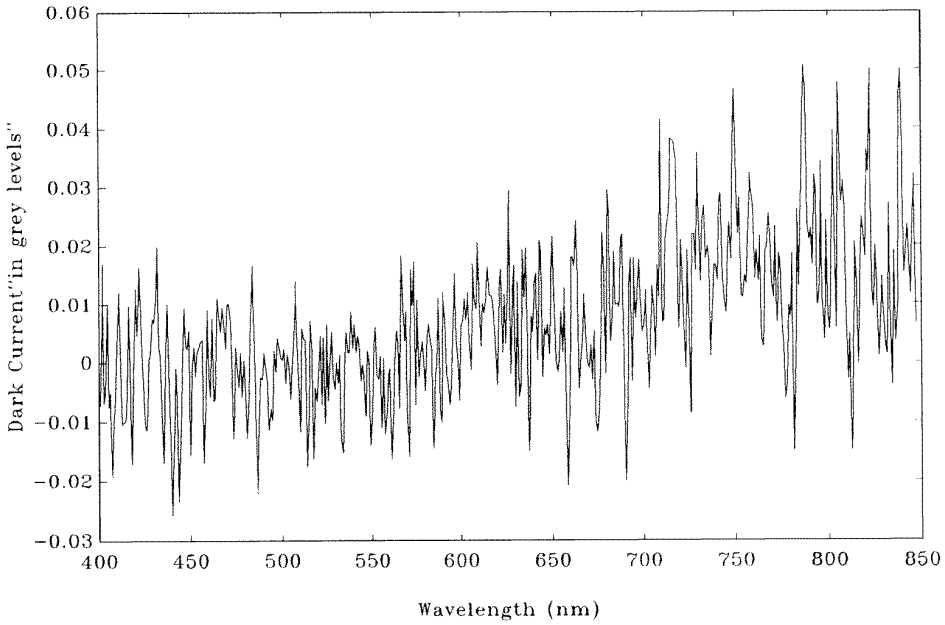

Figure 3. A typical dark current signal from a row of CCD pixels in a single frame.

and detector systems will all be submerged in the ocean to the depth at which measurements are required. A block diagram of the system using only three input channels of the multi-input spectrometer is shown in figure 1.

The functions of the instrument software are to acquire data in the form of CCD image frames and perform integration of spectral data over a specified number of frames. Areas of interest on the image (windows) can be defined to correspond to individual spectral channels. Each window surrounds the spatial (vertical) and spectral dimensions (horizontal) of the focused image onto the CCD. Within each window the computer will be allowed to sample and analyse the data by utilizing the single-frame-advance technique. The average of all the pixels in all the columns in each frame within the window is added to its corresponding average from the next frame. This addition technique can improve the dynamic range significantly. The signal-to-noise ratio increases as the square root of the total number of frames.

Figure 2 shows a typical integrated signal from a tungsten light source with mean integrated dark current subtracted. A typical dark current signal (in digital grey levels) from a row of CCD pixels in a single frame is shown in figure 3.

Independent research [32] has found that a signal as low as 1/25 000 of the camera saturation level can be extracted despite a 20 °C temperature variation using an effective integration time of 10 s. Integration of data vectors within the specified windows is carried out in computer memory and the integrated vectors are stored on disk. The instrument software is based on the MAVIS package from CAPTEC (Computer Applied Techniques Ltd in Ireland).

3. Description of the optical design

The defined measurement requirements demand that the source wavelength for the path transmissivity measurement should include the spectral range 400–800 nm, and the angular divergence of the sampled beam be $<1^\circ$. For the scattering measurement, the sample should be measured at 120°, and the allowed angular divergence of the projected beam is required to be within $\pm 2.5^\circ$. A detailed feasibility study for this instrument system has been carried out and is reported elsewhere [34]. The computations illustrate the capacity of the transmissometer for measuring the spectral beam attenuation coefficient *in situ* across the visible spectrum. Moreover, the scatterometer is expected to perform well in waters with values of scattering coefficient $b > 0.3\ \mathrm{m}^{-1}$. The study assumed that suitable precautions are made to reduce or eliminate excessive background levels due to ambient light.

The optics of the scatterometer and the transmissometer were chosen to accurately define the limits of the solid angle of the measurement. The receivers in this instrument are optical fibres of 200 μm diameter and 0.18 numerical aperture (NA).

The author evaluated a number of modern spectral transmissometer and scatterometer designs based on constraints related to power consumption and accuracy. The general layout of the mechanical and optical design of the preferred transmissometer and the scatterometer subsystems is shown in figure 4. The optical design constitutes three main units:

- Primary projection unit (common to both, the scatterometer and the transmissometer subsystems).
- Azimuth-angle-independent receiver for the measurement of the scattered radiance at 120° (with respect to the primary beam).

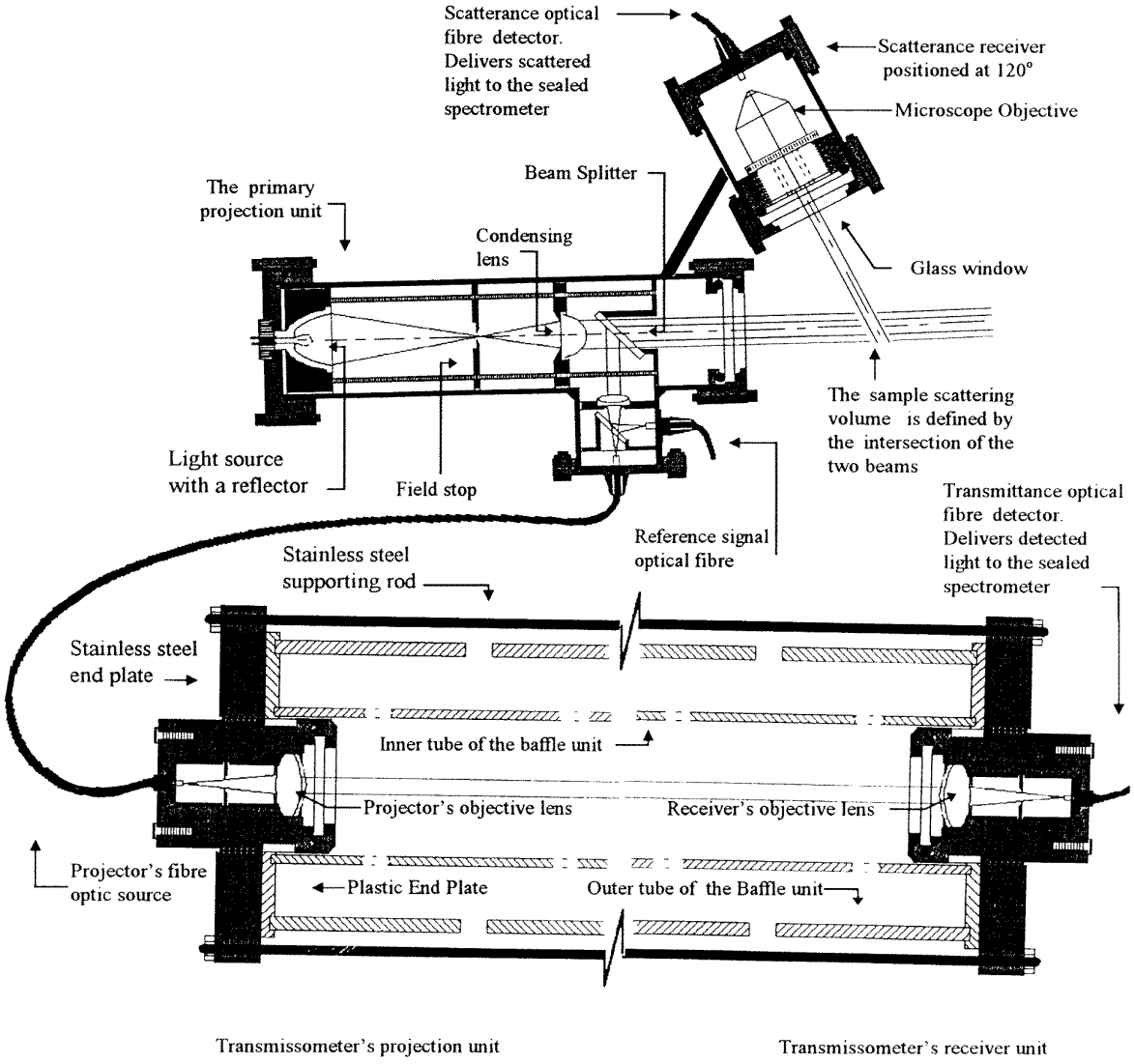

Figure 4. The general layout of the optical and mechanical design of the transmissometer and the scatterometer instrument system. The design constitutes three main units: the primary projection unit, the 120° scatterance receiver, and the transmissometer which consists of a projection unit, a transmittance receiver unit and a baffle unit. Each optical fibre is surrounded by a PVC jacket along its path, and a stress-relief jacket to protect the optical fibre from exceeding its bending limit.

- Transmissometer which consists of a projection unit, a transmittance receiver unit and the baffling unit.

For the measurement of transmittance, a projected beam of highly collimated light is required. The receiver's field of view is determined by the requirement to collect all the flux leaving the projector which has been neither absorbed nor scattered. To reduce the probability of multiple interactions of incident and scattered photons, the water path length in the present design, may be changed from 0.25 m to 0.5 m depending on the optical thickness (cr) of the body of water under consideration. A separate spacer installed between the projector and receiver is required for each of the two measurement path lengths.

3.1. The primary projection unit

Referring to figure 4, a 12 V, 5 W tungsten halogen lamp with a special reflector display without a glass cover (32 mm diameter from inside) designed to transmit heat backwards, focuses a light spot at a field stop having a diameter of 1 mm and located 46 mm away from the reflector's front edge and at the focal plane of the aspheric glass condensing lens. The electric power is driven to the lamp via a bulk-head pressurized water-proof power connector mounted at the back housing of the primary projection unit.

For highly efficient use of the light source; a low f-number aspheric glass condenser lens having a diameter of 18 mm and a short focal length of 12 mm is used in the projector. Aspheric lenses are ideally suited for low f-number and high throughput applications. The clear aperture of the condensing lens was stopped down to 8.35 mm to match the numerical aperture of the reflector display.

The condensing lens forms an image of the field stop at infinity, and a beam of light is formed which

diverges as it leaves the clear aperture of this condensing lens. The angular size of this divergence is determined by the size of the field stop and the focal length of the condensing lens. The beam leaves the condensing lens and passes through a round beamsplitter having a reflection/transmission ratio of 30/70. The transmitted component passes through a high-pressure water-proof glass window of 38 mm diameter and 6 mm glass thickness. This transmitting component forms the primary beam for the scatterometer subsystem. The reflected beam component enters a precision optimized achromatic lens of initial diameter 12 mm and focal length 7 mm. The clear aperture of this lens has been stopped down to 4.32 mm to match the f-number of the receiving optical fibres to reduce unwanted stray light. Having passed through a second round beamsplitter having a reflection/transmission ratio of 30/70; the lens then focuses the reflected and the transmitted images of the field stop at two receiving optical fibres located in two perpendicular focal planes. The reflected component from the beamsplitter is coupled into an optical fibre which carries the reference signal directly to the sealed spectrometer via bulk-head pressurized water-proof connectors. The second optical fibre in the projection unit facilitates the delivery of the transmitted image component which forms the source input to the transmissometer. The other end of this optical fibre is mounted at the focal point of the projector's objective lens of the transmissometer via a bulk-head pressurized water-proof connector mounted at the back of the projector housing. A similar arrangement was made at the receiver side of the transmissometer to transmit the received light signal down a glass fibre and subsequently input to the spectrometer.

All of the optical fibres used have a core diameter of 200 μm and a glass cladding of slightly lower refractive index with 250 μm diameter. Beyond the cladding diameter a protective layer of silicon resin is applied and this, in turn, is finally covered with a Tefzel jacket bringing the outside diameter to 600 μm. Tefzel exhibits many of the chemical and temperature properties of Teflon and would suffice as the final protective layer in the marine environment. However, additional protection was provided by a PVC jacket which surrounds the optical fibre along its length. A stress-relief jacket to protect the optical fibre from exceeding its bending limit is fixed on.

Since the focal lengths of the two lenses in the light projection unit are equal, the field stop will be imaged at the receiving optical fibres at unit magnification. Because the field stop image is larger than the core diameters of the receiving optical fibres; it is the optical fibre throughput that will limit light collection. Sufficient alignment tolerance for the receiving fibres is permitted while assuring image focusing.

3.2. The transmissometer's projection unit

The acceptance half angle of the receiver, θ_{hr}, is related to the effective focal length of the receiver's objective lens, f_{r}, by $\theta_{\mathrm{hr}} = D_{\mathrm{f}}/2f_{\mathrm{r}}$, where D_{f} is the core diameter of the receiving fibre and f_{r} is the effective focal length of the receiver lens.

The primary projection unit provides a small point source of light at the focal point of the transmissometer's projective lens, through an optical fibre of 200 μm core diameter. The objective lens forms an image of the core area of the optical fibre at infinity, and a beam of light is formed which diverges as it leaves the projector. The angular size of this divergence is determined by the core diameter of the projector's optical fibre and the focal length of the objective lens. Light will be emitted from every point on the objective into a cone whose half apex angle is θ_{hr} in radians.

A precision-optimized achromatic lens having a diameter of 18 mm and a focal length of 50 mm has been chosen for the transmissometer's projector unit. An identical lens has also been chosen for the receiver unit. The clear aperture of these lenses as stated by the manufacturer was 16.2 mm.

The projector and the receiver units of this transmissometer employ identical optical fibres and lenses. This implies that the half-angle beam divergence of the projected beam, θ_{hp}, and the half-angle acceptance of the receiver are equal, i.e. $\theta_{\mathrm{hp}} = \theta_{\mathrm{hr}} = D_{\mathrm{f}}/2f = 2$ mrad in air, and about 1.5 mrad ($\cong 0.086^{\circ}$) in water. D_{f} is the core diameter of the source or receiver optical fibre ($= 0.2$ mm) and f is the effective focal length of the lens considered at the projector or receiver of the transmissometer ($= 50$ mm). The clear diameter of the projector's objective lens, D_{p}, was further stopped down to 14.2 mm according to $D_{\mathrm{p}} = D_{\mathrm{r}} - 2\theta_{\mathrm{hp}} r_{\mathrm{max}}$, where $D_{\mathrm{r}} = 16.2$ mm is the beam diameter at the receiver's objective lens (minimum diameter of receiver's aperture stop), $\theta_{\mathrm{hp}} = 2$ mrad is the half-angle beam divergence of the projected beam in air, and $r_{\mathrm{max}} = 0.5$ m is the maximum water path length for transmittance measurements. With this arrangement, the effective f-number of the projector's objective lens is 3.52.

3.3. The transmittance receiver unit

After the beam leaves the objective lens of the projector, and travels the measurement path, it enters through the glass window of the receiver, and then through the objective lens of the transmittance receiver. The entrance aperture of the receiver must be large enough to accept all of the light in the beam, allowing for divergence of the beam plus some clearance. The receiver objective lens forms an image of the core area of the projector's optical fibre in its focal plane. The angular acceptance of the receiver is a function of its receiver diameter, D_{f}, and the focal length of the objective lens, f_{r}. Light entering any point on the receiver objective will pass through the receiver optical fibre only if it enters within the angular limits, θ_{hr}, of the receiver.

3.4. The scatterance receiver

For the measurement of the volume scattering function, $\beta(120^{\circ})$, the field of view of the receiver is such that it only accepts flux which has been scattered by the water at the desired median angle, 120°.

The receiver for the measurement of the scattered radiance at 120° employs a high-quality microscope

objective of numerical aperture 0.17 and effective focal length 14 mm. The microscope objective couples the received scattered radiance into the receiver's optical fibre for subsequent delivery to the sealed spectrometer. The numerical aperture of this microscope objective matches that of the optical fibre. This ensures effective light coupling with minimum losses. The directly transmitted image component through the first beamsplitter forms the primary beam for the scatterometer subsystem. The sample scattering volume is defined through the intersection of the primary beam and the field of view of the scatterance receiver. To reduce excessive background levels due to ambient light, a light trap whose plane is perpendicular to the optical axis of the scatterance receiver can be installed some distance away from the scattering volume along the line of sight of the receiver (not shown in the diagram). This should reduce unwanted ambient background components entering the scatterance receiver.

4. Assembly and mechanical design

4.1. Primary projection unit and scatterance receiver

The water-proof high-pressure housing of the primary projection unit is constructed from two cylindrical iron tubes positioned at right angles to each other (figure 4). The vertical chamber houses the optical components used for deriving the required light monitoring signal and the transmissometer's input signal. The optical components in the primary projection unit have been arranged and mounted onto a cylindrical chassis composed of three screw-type bars and aluminium discs onto which the optical components are held. When the chassis has been fully inserted into the cylindrical iron tube, a seal is obtained by bolting the end plate to the flange and consequently compressing an O-ring between these two surfaces. The microscope objective of the scatterance receiver is housed in a similar iron tube but screwed into position. The optical fibre of the scatterance receiver is mounted onto an O-ring sealed end plate via a bulkhead pressurized water-proof connector.

A suitable marine paint may be applied to protect the outside walls of the tubes from corrosion. A carefully machined aluminium base to receive the curved surface of the reflector display of the primary projection unit is incorporated specifically to effectively dissipate the heat generated from the light source.

4.2. Mechanical design of the transmissometer

The mechanical design of the transmissometer was based on providing a robust, in-line instrument that could take the normal shipboard abuse and maintain its optical alignment. The support structure of the transmissometer is made from stainless steel to withstand the corrosive marine water environment (figure 4).

The projector and the receiver units are mounted in machined heavy stainless-steel cylindrical housings. Approximately the middle part of the outer wall surface of each housing was externally threaded. Each unit was then screwed into a threaded round opening at the centre of a stainless-steel circular end plate. The end plates are accurately separated and aligned parallel with respect to each other by means of four heavy stainless-steel bars screwed onto them.

4.3. Baffling unit of the transmissometer

One of the basic problems in the measurement of the extinction coefficient, c, by a transmissometer system, is the separation of the desired target signal from naturally present and relatively high background ambient light levels which radiate and scatter flux into the sample measurement volume and instrument aperture from all directions. The objective of the c measurement is to obtain the residual flux from a specific geometrical region determined by the instrument field of view and the specified water path length. The geometrical problem of the design of the transmissometer is therefore a problem of spatial purity. The instrument output for a spatially pure measurement is a function of the flux originating from within the specified region and is completely independent of any flux arriving at the instrument aperture from outside that region. The marine background conditions are not easily simulated to compensate for the undesired ambient light. Thus it is necessary to employ a suitable shield on the transmissometer to eliminate the effects of the surrounding light field, and yet allow the rapid exchange of the water measurement volume as the transmissometer is lowered in the ocean from one depth to another. The designed 25 cm water-path length shield consists of two plastic tubes (inner and outer) with holes drilled in the walls of each tube to facilitate rapid exchange of water in the measurement path as shown in figure 4.

The inner tube is assembled in such a way that a hole on its wall is positioned at the centre of the space surrounded by four holes on the outer tube. A black diffuse surface treatment is used on the inner and outer surfaces of both tubes to absorb scattered radiation. Thus scattering from tubing surfaces back into the sample measurement volume is effectively eliminated. Both tubes were maintained in position on the optical axis of the transmissometer by two plastic end plates each having a round opening at its centre. The diameter of the opening is slightly larger than the size of the projector and receiver housings of the transmissometer. The plastic end plates are supported through their round openings on those parts of the housing units on the inner sides of the stainless steel end plates. Two circular grooves were machined in the inner side of each plastic end plate to accommodate the ends of the inner and the outer tubes. The tubes are thus held in position by the plastic end plates. To ensure that no rotation of either of the tubes takes place around the optical axis; resin was applied to the circular grooves of one end plate only. This ensures that the relative geometrical positions of the holes on the inner and the outer tubes are kept permanently in the desired position. If necessary the other end plate can be easily pulled and separated from the tubing for efficient cleaning and maintenance of the inside of either of the tubes. The same principles apply to the 50 cm water-path length shield.

Laboratory testing of a prototype of the transmissometer in air showed that the baffle system, designed to exclude ambient light when the instrument is used in the sea in daylight, works satisfactorily. Although no formal tests have been conducted to determine the flushing time or the extent of biofouling that might take place (particularly on long-time-series deployments), it was clear that there were no areas with inadequate flushing. The design is highly efficient in excluding unwanted background light normally present in the marine environment which is a critical requirement, particularly for a low-power instrument system of the type under consideration. Considering that the design allows for easy and effective cleaning of the baffling around the light path, it is thought that this design of the baffling unit is a promising compromise and would satisfactorily accomplish the purposes for which it was designed.

5. Absolute calibration

5.1. The volume scattering function in absolute units

Ocean optics research and radiative transfer models generally require data in absolute units [37]. This allows the comparison of data collected by different instruments at different times to be made. Absolute calibration provides the relationship between the digital counts recorded by the instrument and the spectral radiance collected and measured over the solid angle of the receiver. Accurate knowledge of the absolute value of the volume scattering function at 120° is required to estimate the backward scattering coefficient, b_b.

In order to determine the volume scattering function of a sample in absolute units, several methods have been presented in the literature. Tyler [38] extends the theoretical analysis of an atmospheric polar nephelometer by Pritchard and Elliott [39] and applies it to the volume scattering function of ocean water. The analysis yields an equation for the volume scattering function, $\beta(\theta, \lambda)$, which requires for its solution a detailed knowledge of the optical properties of a diffusing plastic calibration plate, a somewhat tedious calibration procedure to allow for the dependence of the sample volume and the irradiance input to this volume, and a knowledge of the transmittance of the water used for calibration and the water being measured. Full details of these analyses are well described in Tyler and Austin [40]. The method used by Petzold [11] for the absolute calibration of his field scattering measurements is simple and accurate. It does, however, require two sets of measurements to be made; a transmittance measurement and a scatterance measurement in the desired direction. The transmittance measurement requires use of a calibrated attenuator which lies in the main beam path in the direction $\theta = 0°$ to keep the on-axis measured signal within the range of the detector.

Scattering meters can also be calibrated by comparing the scattering power of a sample measured using the meter, with a known standard, the scattering power of which has been previously established. Since a standard optically pure water is difficult to achieve in practice [41], benzene [42, 43] or commercial spectroscopy grade methanol are often used. The main merits of methanol are: (i) methanol is easily available and relatively pure; (ii) its volume scattering function is approximately two and half times higher than that of water over the whole visible range; this relates to the calibration accuracy and (iii) its refractive index is almost the same as that of water [44].

If the refractive indices of the liquids to be compared are different, corrections are necessary because the volumes from which the scattering is measured and the solid angle within which the scattered light received by the measuring device is contained, vary (since beam spread in different liquids varies).

Coumou [43] has shown that for comparing fluxes of light scattered in different media, the corrections for volume and solid angle can be combined into one refractive index correction. Its value, using cylindrical as well as rectangular liquid cells is equal to the square of the ratio of the refractive indices. Similar conclusions are given by Brice *et al* [45]. For two different liquids (a sample and a standard), the result is

$$V_{\mathrm{std}}\Omega_{\mathrm{std}}[n_{\mathrm{std}}(\lambda)]^2 = V\Omega[n(\lambda)]^2 \tag{2}$$

where V is the scattering volume of a sample contained in a cell, Ω is the solid angle over which the scattered light from sample volume is collected and measured and $n(\lambda)$ is the refractive index of the sample. The subscript 'std' stands for a standard liquid.

Using equation (2), it can be shown that the volume scattering function at 120° (in absolute units) is given by

$$\beta(120°, \lambda) = \left[\frac{S(120°, \lambda)}{S_{\mathrm{std}}(120°, \lambda)}\right]\left[\frac{\exp(c(\lambda)\, r)}{\exp(c_{\mathrm{std}}(\lambda)\, r)}\right] \times \left[\frac{n(\lambda)}{n_{\mathrm{std}}(\lambda)}\right]^2 \beta_{\mathrm{std}}(120°, \lambda) \tag{3}$$

where $S(120°, \lambda)$ and $S_{\mathrm{std}}(120°, \lambda)$ are the instrument output corrected signals (dark current subtracted) in response to the measurement of the scattered radiance in the direction 120° for the sample (sea water in our case) and the standard, respectively. The measurement $S_{\mathrm{std}}(120°, \lambda)$ can be performed by lowering the scatterometer into a calibration tank containing a standard liquid of known $\beta_{\mathrm{std}}(120°, \lambda)$. Evaluation of $\beta(120°, \lambda)$ in absolute units requires knowledge of the refractive indices of both the standard and the sample at the wavelength of interest. The spectral attenuation coefficients of the standard and the sample, $c_{\mathrm{std}}(\lambda)$ and $c(\lambda)$, must also be determined in absolute units. The ratio $[\exp(c(\lambda)\, r)/\exp(c_{\mathrm{std}}(\lambda)\, r)]$ is inserted into equation (3) to compensate for the attenuation losses suffered by the scattered beams in traversing a length r both in the sample and in the standard; r is the length between the midpoint of the scattering volume and the scatterance receiver. The same ratio also accounts for changes in the transparency of the water and between the water and the standard. Equation (3) assumes that the medium is optically homogeneous within the path length of measurement. It is valid under the conditions of a sufficiently small solid angle receiver and the same irradiance on the scattering volume of the sample and of the standard.

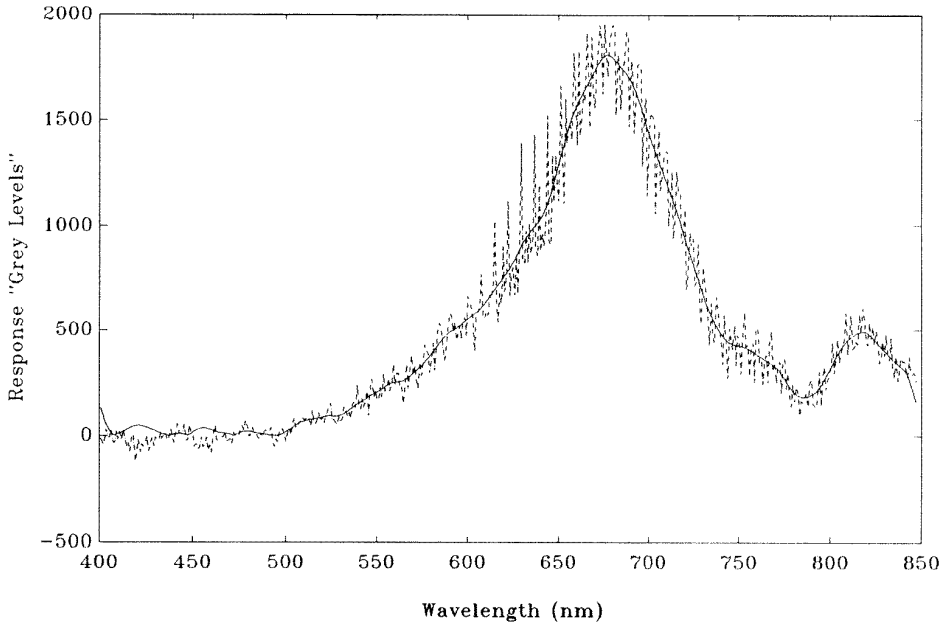

Figure 5. A typical integrated low light level noisy signal with its corresponding filtered one (full curve). The signal-to-noise ratio below 500 nm can be improved by employing a light source with an improved output in the blue–green part of the spectrum and/or a CCD detector with a greater blue response. The distortion (tail) at the left end points of the filtered signal (which may be disregarded) is a side effect of digital filtering.

In order to calculate the absolute scattering power of a standard, several methods have been presented [39, 41, 44, 46]. The calibration of the standard can also be conducted in the laboratory by immersing a general angle calibration scatterometer in the reference liquid and following a procedure similar to that used by Petzold [11] for the absolute calibration of his field scattering measurements (i.e. by extending Petzold's analysis to the problem of deriving the absolute calibration of a standard in a large calibration tank in the laboratory).

5.2. The beam attenuation coefficient in absolute units

The beam attenuation coefficient, $c(\lambda)$, in absolute units can be determined by measuring the relative flux transmitted over two path lengths; $r_1 = 0.5$ m and $r_2 = 0.25$ m. Using this method, $c(\lambda)$, can be calculated from

$$c(\lambda) = -\frac{\ln[S_2(\lambda)/S_1(\lambda)]}{r_2 - r_1} \tag{4}$$

where $S_1(\lambda)$ and $S_2(\lambda)$ are the corrected signals (dark current subtracted), recorded by the instrument in response to the measurement of the residual flux of a transmissometer's projected beam in a body of water over the two path lengths r_1 and r_2. Sources of errors due to the determination of the instrument profile, CCD responsivity, gain and optical losses, are thus eliminated, and need not be known. This method can be the most accurate means of calibration. It does, however, require two sets of measurements to be made.

Absolute calibration of field transmittance data can also be accomplished by comparing the corrected measured field signals with measurements taken by the same transmissometer on a working transmittance standard, the spectral attenuation coefficient of which has previously been established in the laboratory. The spectral reference data of the standard and the measured field profiles can then be utilized to derive the beam attenuation coefficient of a field measurement in absolute units. This calibration procedure can easily be performed each time the instrument is operated. This calibration strategy requires careful cleaning of the instrument to avoid changing the transmittance of the standard; placing an instrument into a working transmittance standard will usually introduce some contamination.

6. Summary

The optical design of the system described in this paper is directed toward maintaining adequate light source efficiency and detector sensitivity to perform accurate simultaneous scatterance and transmittance measurements, without the need for complex and power-consuming arrangements. This paper reveals that a spectral scatterometer and a spectral beam attenuation meter is feasible from a technical perspective. It is thought that the working version of the system can be utilized for general oceanographic applications.

Significant effort has been expended on fine tuning the final design and arriving at a compact, sturdy underwater package. The mechanical design was based on providing a robust rugged instrument that could take the typical shipboard abuse and maintain its optical alignment. The instrument's modular construction allows for future modification or alteration of its present performance.

The main features and improvements of this versatile system design over many existing instruments include, the

relatively low power requirements, significant improvement can be achieved in the instrument dynamic range and signal-to-noise ratio using the frame-addition technique, the transmissometer is not sensitive to ambient light, permitting measurements to be made from surface to depths of 100 m at any time of the day. Furthermore, other optical collectors can be integrated into the same spectrometer to yield comprehensive simultaneous spectral signatures of optical properties, and provide basic research data essential for future global estimates of marine constituents.

7. Further developments

Figure 5 shows a low light level noisy signal with its corresponding filtered one (full curve) using a moving average digital low-pass filter. These raw data are taken from results of first trials obtained from preliminary testing, of a prototype of the transmissometer, in a water tank, in the laboratory. Although the results obtained from the first trials are inadequate to give a guide to instrument performance, the figure suggests that in conditions of low light levels, the response in the blue–green region of the spectrum could be improved by employing a camera system with greater blue response in order to improve signal quality below 500 nm. Well planned and carefully executed testing procedures are required to provide a guide to instrument performance. *In situ* experimental confirmation is also indispensable to establish complete performance specifications of this instrument system. Implementation of high-precision algorithms for temperature calibration and for dark current subtraction of the CCD detector of the spectrometer to improve the capabilities for measurement of very low light levels is also a critical requirement.

Acknowledgments

The work described in this paper is part of the author's PhD thesis. The paper is based on work carried out by the author in the Physics Department of University College Dublin (UCD) as a component for the development of the Marine Radiometric Spectrometer (MARAS). The project has been supported from the UCD under the Marine Science and Technology (MAST) programme of the Commission of the European Communities, contract number 0007-C and MAS2-CT92-0020.

References

[1] Kirk J T O 1989 *Limnol. Oceanogr.* **34** 1410–25
[2] O'Mongain E *et al* 1997 *Opt. Laser Technol.* **29** 41–4
[3] Voss K J and Austin R W 1993 *J. Atmos. Oceanic Technol.* **10** 113–21
[4] Buiteveld H, Hakvoort J H M and Donze M 1994 *Proc. SPIE* **2258** 174–83
[5] Pegau W S, Zaneveld J R V and Voss K J 1995 *J. Geophys. Res.* **100 C7** 13193–9
[6] Bricaud A, Roesler C and Zaneveld J R V 1995 *Limnol. Oceanogr.* **40** 394–410
[7] Duntley S Q 1963 *J. Opt. Soc. Am.* **53** 214–32
[8] Smith R C 1974 *Optical Aspects of Oceanography* ed N G Jerlov and E Nielsen (London: Academic)
[9] Dera J and Sagan S 1990 *Oceanologia* **28** 76–101
[10] Voss K J 1992 *Limnol. Oceanogr.* **37** 501–9
[11] Petzold T J 1972 Rep. Visibility lab. (Scripps Oceanography Institute, University of California, References 72–78)
[12] Shannon J G 1975 *Proc. SPIE* **64** 3–11
[13] Austin R W and Petzold T J 1977 *Light in the Sea* ed J E Tyler (Stroudsbury: Dowden, Hutchinson & Ross)
[14] Petzold T J and Austin R W 1968 *SPIE* **12** 133–7
[15] Austin R W and Petzold T J 1975 *Proc. SPIE* **64** 50–61
[16] Carder K L, Steward R G and Payne P R 1984 *Proc. SPIE* **489** 325–34
[17] Caimi F M, Tusting R F and Kennedy G 1984 *Proc. SPIE* **489** 364–74
[18] Carder K L, Steward R G, Peacock T G, Payne P R and Peck W 1988 *Ocean Optics IX, SPIE* **925** 189–95
[19] Svensson S, Ekstrom C, Ericson B and Lexander J 1988 *Proc. SPIE* **925** 203–12
[20] Borgerson M J, Bartz R, Zaneveld J R V and Kitchen C 1990 *Proc. SPIE* **1302** 373–85
[21] Moore C, Bruce E J and Pegau W S 1996 *Proc. SPIE* **2963** 435–9
[22] Hakvoort H and Doerffer R 1996 *Proc. SPIE* **2963** 435–9
[23] Voss J M and Smart J H 1994 *Proc. SPIE* **2258** 116–22
[24] Preisendorfer R W and Mobley C D 1984 *Limnol. Oceanogr.* **25** 903–29
[25] Aas E 1987 *Appl. Opt.* **26** 2095–101
[26] Stavn R and Weidemann A D 1989 *Limnol. Oceanogr.* **34** 1426–41
[27] Hojerslev N K 1986 *Landolt–Bornstein Encyclopaedia* vol 3a, ed J Sundermann (Berlin: Springer)
[28] Kullenberg G 1984 *Deep Sea Res.* **31** 295–316
[29] Oishi T 1990 *Appl. Opt.* **29** 4658–65
[30] Maffione R A, Dana D R and Honey R C 1991 *Underwater Imaging, Photography and Visibility, SPIE* **1537** 173–84
[31] Schwarz J, Weeks A, Trundle K and Robinson I 1996 *Proc. SPIE* **2963** 614–9
[32] Moore K, O'Mongain E, Plunkett S, Doerffer R and Bree M 1993 *SPIE Proc.* **2048** 153–65
[33] Moore K 1994 *PhD Thesis* National University of Ireland (NUI)/(UCD)
[34] Zalloum O H Y 1994 *PhD Thesis* National University of Ireland (NUI)/(UCD)
[35] Bree M 1995 *PhD Thesis* National University of Ireland (NUI)/(UCD)
[36] O'Malley M and O'Mongain E 1992 *Opt. Eng.* **31** 522–6
[37] Mueller J L and Austin R W 1992 *Ocean Optics Protocols for SeaWIFS Validation* vol 5 NASA Technical memorandum 104566
[38] Tyler J E 1963 *Appl. Opt.* **2** 245–8
[39] Pritchard B S and Elliott W G 1960 *J. Opt. Soc. Am.* **50** 191–202
[40] Tyler E J and Austin R W 1964 *Appl. Opt.* **3** 613–20
[41] Morel A 1974 *Optical Aspects of Oceanography* ed N G Jerlov and E S Nielsen (London: Academic)
[42] Pike E R, Pomeroy W R M and Vaughan J M 1975 *J. Chem. Phys.* **62** 3188–92
[43] Coumou D J 1960 *J. Colloid Soc.* **15** 408–17
[44] Oishi T 1987 *Light Scattering and Polarisation by Suspended Particle Matter in Sea Water* Report, Institute of Physics and Oceanography no 49, University of Copenhagen
[45] Brice B A, Halwer M and Speiser R 1950 *J. Opt. Soc. Am.* **40** 768–78
[46] Aas E 1979 *The Calibration of a Scatterance and Fluorescence Meter* Report, Institute of Geophysics no 40, University of Oslo